(12) INTERNATIONAL APPLICATION PUBLISHED UNDER THE PATENT COOPERATION TREATY (PCT)

(19) World Intellectual Property Organization
International Bureau

(43) International Publication Date
3 November 2016 (03.11.2016)

WIPO | PCT

(10) International Publication Number
WO 2016/176415 A1

(51) International Patent Classification:
A61B 3/02 (2006.01) *A61B 3/14* (2006.01)
A61B 3/12 (2006.01) *A61B 3/00* (2006.01)
A61B 13/00 (2006.01)

(21) International Application Number:
PCT/US2016/029717

(22) International Filing Date:
28 April 2016 (28.04.2016)

(25) Filing Language: English

(26) Publication Language: English

(30) Priority Data:
62/154,490 29 April 2015 (29.04.2015) US

(71) Applicants: **OHIO STATE INNOVATION FOUNDATION** [US/US]; 1524 North High Street, Columbus, Ohio 43201 (US). **ARIZONA BOARD OF REGENTS ON BEHALF OF THE UNIVERSITY OF ARIZONA** [US/US]; 220 West Sixth Street, 4th Floor, Tucson, Arizona 85701 (US).

(72) Inventors: **DOBLE, Nathan**; 7650 Johntimm Court, Dublin, Ohio 43017 (US). **BLANCO, Leonardo**; 73 rue Monge, 75005 Paris (FR). **CODONA, Johanan**; The University of Arizona, 933 N. Cherry Ave., Tucson, Arizona 85721 (US). **MORRIS, Hugh**; 1895 Suffolk Road, Upper Arlington, Ohio 43221 (US).

(74) Agents: **PAPROCKI, Andrew** et al.; 100 East Wisconsin Avenue, Suite 3300, Milwaukee, Wisconsin 53202 (US).

(81) Designated States *(unless otherwise indicated, for every kind of national protection available)*: AE, AG, AL, AM, AO, AT, AU, AZ, BA, BB, BG, BH, BN, BR, BW, BY, BZ, CA, CH, CL, CN, CO, CR, CU, CZ, DE, DK, DM, DO, DZ, EC, EE, EG, ES, FI, GB, GD, GE, GH, GM, GT, HN, HR, HU, ID, IL, IN, IR, IS, JP, KE, KG, KN, KP, KR, KZ, LA, LC, LK, LR, LS, LU, LY, MA, MD, ME, MG, MK, MN, MW, MX, MY, MZ, NA, NG, NI, NO, NZ, OM, PA, PE, PG, PH, PL, PT, QA, RO, RS, RU, RW, SA, SC, SD, SE, SG, SK, SL, SM, ST, SV, SY, TH, TJ, TM, TN, TR, TT, TZ, UA, UG, US, UZ, VC, VN, ZA, ZM, ZW.

(84) Designated States *(unless otherwise indicated, for every kind of regional protection available)*: ARIPO (BW, GH, GM, KE, LR, LS, MW, MZ, NA, RW, SD, SL, ST, SZ, TZ, UG, ZM, ZW), Eurasian (AM, AZ, BY, KG, KZ, RU, TJ, TM), European (AL, AT, BE, BG, CH, CY, CZ, DE, DK, EE, ES, FI, FR, GB, GR, HR, HU, IE, IS, IT, LT, LU, LV, MC, MK, MT, NL, NO, PL, PT, RO, RS, SE, SI, SK, SM, TR), OAPI (BF, BJ, CF, CG, CI, CM, GA, GN, GQ, GW, KM, ML, MR, NE, SN, TD, TG).

Published:

— *with international search report (Art. 21(3))*

(54) Title: RAPID MEASUREMENT OF INDIVIDUAL CONE PHOTORECEPTOR POINTING FOR EVALUATION OF EYE HEALTH USING FOCUS DIVERSITY

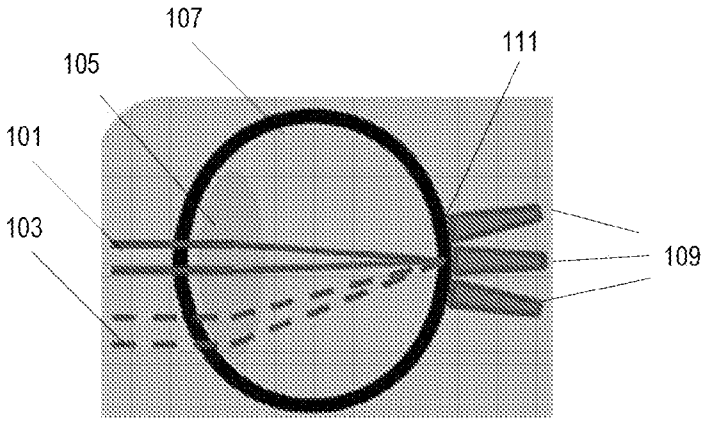

FIG. 1A

(57) Abstract: Systems and methods are described for measuring angular direction of individual photoreceptors in an eye. A light source is projected through the pupil of the eye onto the retina. An image of the light reflected back from the plurality of photoreceptors is captured at a first focal depth and then at a second focal depth, where the first focal depth is different than the second focal depth. At least one individual photoreceptor is identified in both images and a lateral difference of the position of the identified photoreceptor is measured. The angular direction of the photoreceptor is then calculated based on the measured lateral difference.

WO 2016/176415 A1

RAPID MEASUREMENT OF INDIVIDUAL CONE PHOTORECEPTOR POINTING FOR EVALUATION OF EYE HEALTH USING FOCUS DIVERSITY

CROSS-REFERENCE TO RELATED APPLICATION(S)

[0001] This application claims the priority of U.S. Provisional Patent Application No. 62/154,490, filed on April 29, 2015, the entire contents of which is fully incorporated herein by reference.

BACKGROUND

[0002] The present invention relates to systems and methods for evaluating ocular and potentially systemic health based on the pointing direction of cone photoreceptors.

[0003] The Stiles-Crawford Effect of the First Kind (SCE-I) describes how rays of light entering near the center of the eye's pupil appear brighter to an observer than rays incident near the periphery. Fig. 1A illustrates this effect by showing a first centered ray of light 101 and a second off-center ray of light 103 entering the pupil 105 of the eye 107 and reaching photoreceptor cones 109 at the retina 111. The graph of Fig. 1B shows perceived intensity of the light (y-axis) as a function of displacement from center of the pupil (x-axis). As shown in Fig. 1B, the perceived intensity of the first light ray 101 is much higher (point 113) than the perceived intensity of the second light ray 103 (point 115 in the graph). This effect is due to the waveguide properties of the cone photoreceptors, and it has been demonstrated that various eye conditions such as amblyopia, retinal detachment and retinal degeneration have an altered SCE-I function.

[0004] Photoreceptor tilt can be measured based on the SCE-I. Prior measurement of the photoreceptor tilt has typically been performed psychophysically as a subjective comparison of the perceived intensity of a flickering stimulus relative to a static background. The stimulus would be moved across the subject's pupil to measure the luminance efficiency as a function of pupil eccentricity. This subjective method required lengthy experimental sessions and a high degree of concentration and cooperation from test subjects, making it impractical to be a routine clinical measurement technique.

[0005] Other, more time efficient techniques analyze the intensity distribution of reflected light at the pupil plane. The distribution of light reflected back from the retina, illuminated from a small source, is measured in the plane of the eye's pupil. The distribution

of the reflected light returning from the retina presents a peaked profile. These pupil plane reflectometric techniques similarly provide an estimate of the pupil location towards which the photoreceptors are pointing; however the directionality is greater (higher rho values) than that measured psychophysically. Both of these approaches measure the properties of an ensemble of cones and are incapable of measuring the directionality of individual cones.

SUMMARY

[0006] Various embodiments of the invention provide a rapid technique for measuring directionality of single cone photoreceptors. In a healthy eye, all of the cone photoreceptors generally point towards the center of the pupil or with a slight nasal bias, while in diseased eyes, there is more disarray. Measurement of the disarray may be an early indicator of retinal and / or systemic disease including, for example, age-related macular degeneration (AMD). In some medical conditions, cone disarray may be an observable precursor to cell death (i.e., reductions in photoreceptor density). When cone disarray is detected using the methods and techniques described in this disclosure, drug therapies and other treatment types might be prescribed to preserve photoreceptor function. Earlier diagnosis leads to earlier treatment and potentially improved treatment outcomes.

[0007] Some embodiments use adaptive optics (AO) to overcome the aberrations of the eye allowing for resolution at the level of individual cone photoreceptors. However, other embodiments are able to image individual cone photoreceptors without adaptive optics using imaging devices such as, for example, a non-AO fundus camera or a scanning laser ophthalmoscope (SLO).

[0008] Individual cones can be imaged and their apparent location measured relative to their neighbors. Each of these cones can be regarded as individual optical fibers that reflect light in a well-defined beam towards the center of the eyes pupil. An imaging system captures images of the retina at one or more focus positions. This can be accomplished in rapid succession, but the speed of acquisition does not affect the resulting measurement. By comparing the apparent lateral positions of the cones with changing focal position the directionality or pointing of individual cones can be determined.

[0009] Whereas existing techniques are subjective in nature and can take around 40 minutes to complete, the techniques described herein provide objective analysis and multiple

images at various focal positions can be acquired in just a few seconds. Capturing multiple measurements at a number of retinal locations provides a move complete sample for diagnosis of potential disarray. These techniques and systems can be developed as a stand-alone camera system or may be incorporated into other optical imaging systems including, but not necessarily limited to, fundus cameras, scanning laser ophthalmoscopes, or an OCT imaging device.

[0010] In one embodiment, the invention provides a method of measuring angular direction of individual photoreceptors in an eye. A light source is projected through the pupil of the eye onto the retina. An image of the light reflected back from the plurality of photoreceptors is captured at a first focal depth and then at a second focal depth, where the first focal depth is different than the second focal depth. At least one individual photoreceptor is identified in both images and a lateral difference of the position of the identified photoreceptor is measured. The angular direction of the photoreceptor is then calculated based on the measured lateral difference. In some embodiments, the focal depth is adjusted using an adaptive optics (AO) mechanism (e.g., a lens or a mirror) while, in other embodiments, the focal depths is adjusted using a non-AO mechanism (e.g., a linearly moveable lens).

[0011] Other aspects of the invention will become apparent by consideration of the detailed description and accompanying drawings.

BRIEF DESCRIPTION OF THE DRAWINGS

[0012] Fig. 1A is a cross-sectional schematic view of light being projected into an eye.

[0013] Fig. 1B is a graph of the SCE-I effect on the eye of Fig. 1A.

[0014] Fig. 2 is a graph of the effect of focus diversity for a centered cone photoreceptor and for an angled cone photoreceptor.

[0015] Fig. 3A is a cross-sectional schematic view of a method of a focal plane adjustment in an eye for measuring cone angle using focus diversity.

[0016] Fig. 3B is an overlaid view of the output of a camera system demonstrating lateral movement of reflected light from a cone photoreceptor.

[0017] Fig. 4 is a flowchart of a method for measuring angle of individual cone photoreceptors using focus diversity.

[0018] Fig. 5 is a schematic diagram of a system for measuring angle of individual cone photoreceptors using the method of Fig. 4.

DETAILED DESCRIPTION

[0019] Before any embodiments of the invention are explained in detail, it is to be understood that the invention is not limited in its application to the details of construction and the arrangement of components set forth in the following description or illustrated in the following drawings. The invention is capable of other embodiments and of being practiced or of being carried out in various ways.

[0020] As discussed above, Figs. 1A and 1B illustrate a mechanism for observing tilt of a photoreceptor using the Stiles-Crawford Effect of the first kind (SCE-I). Using an imaging system of sufficient quality (i.e., resolution) to image the location of single cones relative to their neighbors, it is possible to measure the tilt of individual cone photoreceptors by acquiring images while displacing the entrance pupil over the subject's pupil. By comparing the intensities of the individual cones imaged as the entrance pupil is displaced, one can compute the pointing direction for each imaged cone.

[0021] It has been demonstrated that various eye conditions and diseases have an altered SCE-I function. In myopic eyes, a systematic nasal shift in the peak position of the SCE-I function in the nasal retina with an increase in myopia has been reported (see, e.g., Choi, S.S., Garner, L.F., & Enoch, J.M. (2003). The relationship between the Stiles-Crawford effect of the first kind (SCE-I) and myopia. *Ophthalmic and Physiological Optics, 23* (5), 465-472, and Choi, S.S., Enoch, J.M., & Kono, M. (2004). Evidence for transient forces/strains at the optic nerve head in myopia: repeated measurements of the Stiles-Crawford effect of the first kind (SCE-I) over time. *Ophthalmic Physiol Opt, 24* (3), 194-206). Changes in the SCE-I function have also been found in a number of ocular diseases such as central serous chorioretinopathy (see, e.g., Smith, V.C., Pokorny, J., & Diddie, K.R. (1978). Color matching and Stiles-Crawford effect in central serous choroidopathy. *Mod Probl Ophthalmol, 19*, 284-295), retinitis pigmentosa (see, e.g., Birch, D.G., Sandberg, M.A., & Berson, E.L. (1982). The Stiles-Crawford effect in retinitis pigmentosa. *Invest Ophthalmol Vis Sci, 22* (2), 157-

164), age-related macular degeneration (see, e.g., Kanis, M.J., Wisse, R.P.L., Berendschot, T.T.J.M., van de Kraats, J., & van Norren, D. (2008). Foveal cone-photoreceptor integrity in aging macula disorder. *Investigative Ophthalmology & Visual Science, 49* (5), 2077-2081), and a range of other retinal conditions (see, e.g., Smith, V.C., Pokorny, J., & Diddie, K.R. (1988). Color matching and the Stiles-Crawford effect in observers with early age-related macular changes. *Journal of the Optical Society of America a-Optics Image Science and Vision, 5* (12), 2113-2121; Bedell, H.E., Enoch, J.M., & Fitzgerald, C.R. (1981). Photoreceptor orientation. A graded disturbance bordering a region of choroidal atrophy. *Arch Ophthalmol, 99* (10), 1841-1844; Keunen, J.E., Smith, V.C., Pokorny, J., & Mets, M.B. (1991). Stiles-Crawford effect and color matching in Stargardt's disease. *American Journal of Ophthalmology, 112* (2), 216-217; Lakshminarayanan, V., Bailey, J.E., & Enoch, J.M. (1997). Photoreceptor orientation and alignment in nasal fundus ectasia. *Optom Vis Sci, 74* (12), 1011-1018; and Lardenoye, C.W., Probst, K., DeLint, P.J., & Rothova, A. (2000). Photoreceptor function in eyes with macular edema. *Invest Ophthalmol Vis Sci, 41* (12), 4048-4053). Changes in SCE-I function have also been linked to diabetic retinopathy (see, e.g., Bresnick, G.H., Smith, V., & Pokorny, J. (1981). Visual function abnormalities in macular heterotopia caused by proliferative diabetic retinopathy. *American Journal of Ophthalmology, 92* (1), 85-102). Because SCE-I has its origin at the retina, techniques that detect changes in photoreceptors could be used, for example, to diagnose and monitor patients with retinal diseases at a much earlier stage.

[0022] Fig. 2 illustrates an example of a technique, as implemented in some of the systems and methods of this disclosure, utilizing the principle of focus diversity to determine a pointing direction of a photoreceptor (for example, a cone photoreceptor) by comparing the lateral position of imaged cones as the focus of an imaging device is changed. Consider an imaging system designed such that points on the object plane (retinal plane RP) are conjugate to points in the nominal focal plane F0. When a camera sensor is placed in the F0 plane, point sources on RP will appear 'in focus' with the most compact PSFs. In Fig. 2, two cones are shown emitting narrow beams from the RP plane, one oriented along the optical axis and the other with a relative tilt. Both beams form compact images in the focal plane F0.

[0023] In graph (a) of Fig. 2, the narrow beam (shaded) is parallel with the overall optical axis and arrives at the focal plane still parallel with the optical axis. This is true for all RP points since the imaging system is designed to be jointly telecentric in the object and image

spaces. If the camera were 'defocused' by moving it to another plane, say F1 or F2, the beam's image would become broader, but would not shift in lateral position. The situation is different when the narrow beam leaves RP in a tilted direction (e.g., due to photoreceptor disarray) as in the example of graph (b) of Fig. 2. The image is still formed at the same position in F0, but, in other defocused planes, the image is both broadened and shifted.

[0024] Fig. 3A and 3B provide a specific example of this effect on an eye and illustrate one example of a technique for monitoring and detecting this effect. As shown in Fig. 3A, a light source is projected into the pupil of a patient's eye and the light is reflected back by each of three individual cone photoreceptors 109. The focus of a camera imaging system is then adjusted to observe the reflected light at two different focal depths shown in Fig. 3A as Plane 1 and Plane 2. As shown in Fig. 3B, the first cone appears in the same location 401 in both the first focus position and in the second focus position. However, the position of the second cone appears to move laterally from location 402A in the first focal depth to location 402B in the second focal depth. Similarly, the position of the third cone appears to move from location 403A to location 403B.

[0025] As such, it can be concluded that the first cone is positioned at an angle that is substantially collinear with the imaging axis. However, the second and third cones are positioned at other angles relative to the imaging axis. The apparent lateral movement of the cones in the images acquired at different focal depths can be used to calculate an angle of each cone relative to the imaging axis.

[0026] Fig. 3A also illustrates one specific example of a mechanism for adjusting the focus of the imaging system using a deformable mirror 201 and a focusing lens 203 positioned between the deformable mirror and the cone photoreceptors 109. When the deformable mirror 201 is controllably deformed into a first condition (represented by the solid, curved line), the imaging system is focused at the first plane (Plane 1) as indicated by the intersection at Plane 1 of the solid lines extending from the deformable mirror 201. The deformable mirror 201 is then controllably deformed into a second condition (represented by the substantially straight dashed line) thereby focusing the imaging system at the second plane (Plane 2) as indicated by the intersection at Plane 2 of the dashed lines extending from the deformable mirror 201. As such, as illustrated in the example of Fig. 3A, the focus of the imaging system can be adjusted in some implementations using a deformable mirror such as in an adaptive optics (AO) system. However, as discussed in further detail below, in other

implementations, the focus of the imaging system can be adjusted to capture images of the light reflected from the photoreceptors at multiple different focal depths using other types of AO and non-AO focusing mechanism.

[0027] Fig. 4 illustrates a specific example of the processing steps involved in determining the angle of each individual cone photoreceptor relative to an imaging axis. Retinal images are rapidly acquired at 11 focal positions over a physical depth range of ±40 μm in the subject's retina, with 5 retinal images being acquired at each position. An image is captured (step 501) and is repeated until five retinal images have been acquired at a given position (step 503). The imaging system then changes the focal depth (step 507) and repeats the image acquisition step (steps 501 and 503) until five images have been captured at each of 11 focal depth positions (step 505). It is noted that, although the example of Fig. 4 captures five images at each of 11 different focal positions, other implementations may capture more or fewer images at each position and may utilize more or fewer distinct focal positions.

[0028] The 55 images were then registered together (compensating for any shift, rotation and magnification changes between images). The 5 images acquired at the same depth were averaged to improve the signal-to-noise ratio and the contrast of the cones (step 509). The final stack consisted of 11 images, each of them corresponding to a different depth in the retina.

[0029] The cones on each image were then identified with an automated custom MATLAB® routine and the cones in each image were matched (step 511). A cone identified at one depth and a cone identified at another depth are considered to be the same cone if the distance between the two is smaller than a threshold distance, typically 3-4 pixels. If the distance was more than this threshold distance, they were not considered to be the same cone.

[0030] The coordinates of each identified cone were automatically measured on every image allowing measurement of the apparent relative lateral displacement of each cone as the depth is scanned (step 513). Since the axial distance δF between two images and the lateral displacement of the cones on different images are known, the relative angle that the cones subtend with respect to the average pointing direction of the ensemble in the field of view (FOV) can be computed. The focus diversity data, however, only gives the relative pointing angle between the individual cones identified on the images. To obtain the overall pointing direction of the ensemble that are imaged, simultaneous pupil intensity images can also be

acquired using the same light source (e.g., a 680nm light source) with a camera conjugate with the pupil plane of the subject.

[0031] Fig. 5 illustrates a specific example of a system configured to perform the method of Fig. 4. An AO Flood Illuminated Retinal Camera is used to acquire the retinal images. A bleaching source mercury arc lamp 601, an SLD imaging source 603, a fixation target 605, a WFS beacon 607, an alignment laser 609, and various associated optics are configured to project light into the subject's eye pupil 611 to illuminate the cone photoreceptors. A pupil camera 613 monitors the pupil of the subject and a deformable mirror 615 is used to control the conjugate plane by adding a known and controlled amount of defocus to the wave-front. A Shack Hartmann Wavefront Sensor 617 and a Science Camera 621 are used to capture images of the reflected light from the cones. A filter 619 blocks IR before the light reaches the Science Camera 621. A series of images captured by the Science Camera 621 are stored for later analysis. Each image recorded is the image of the irradiance at the conjugate plane of the sensor in the retina (e.g., Plane 1 and Plane 2 as illustrated in Fig. 3A).

[0032] Adaptive optics (AO) systems – such as, for example, the RTX1 retinal camera by Imagine Eyes) – typically have a field of view ranging from 1-4 degrees. However, with proper registration, multiple images are combined to apply the focus diversity methods described above to a much wider field of view. Furthermore, other imaging devices that do not utilize adaptive optics – such as, for example, a scanning laser ophthalmoscope – can be used to image individual cones over a field of view of 5.5 degrees. The systems and methods described above can utilize other imaging devices and techniques to apply the focus diversity technique without necessarily including adaptive optics. In some such systems, the focus of the imaging system can be adjusted by mechanically moving a lens linearly along an optical pathway between the camera/imaging device and the eye of the imaging subject. In other implementations, the focus of the imaging system can be adjusted by other mechanisms including, for example, electro-optic lenses, water-filled lenses, and liquid crystal devices.

[0033] The focus diversity method allows for a very rapid measurement of the pointing direction of individual cones in the field of view of a camera. The computation cost and algorithmic complexity is not significantly increased and the accuracy of the method is comparable to previous techniques. Results obtained on a cone-per-cone basis are in good agreement with measurements made on the same subjects with other photoreceptor tilt measuring techniques.

[0034] Thus, the invention provides, among other things, a non-invasive method of measuring angle positioning of individual cone photoreceptors using focus diversity. Various features and advantages of the invention are set forth in the following claims.

CLAIMS

What is claimed is:

1. A method of measuring angular direction of individual photoreceptors in an eye, the method comprising:

projecting a light from a light source through a pupil of the eye onto a retina of the eye;

capturing an image of light reflected back from a plurality of photoreceptors at a first focal depth;

capturing an image of light reflected back from the plurality of photoreceptors at a second focal depth, the second focal depth being different than the first focal depth;

identifying at least one individual photoreceptor in the image captured at the first focal depth and in the image captured at the second focal depth;

measuring a lateral difference of a position of the identified at least one individual photoreceptor between the image captured at the first focal depth and the image captured at the second focal depth; and

calculating an angular direction of the at least one individual photoreceptor based on the measured lateral difference.

2. The method of claim 1, wherein capturing an image of light reflected back from the plurality of photoreceptors includes capturing an image by an imaging device capable of imaging individual photoreceptors.

3. The method of claim 2, wherein the imaging device is one selected from a group consisting of an optical-coherence tomography system, a scanning laser ophthalmoscope, and a fundus camera.

4. The method of claim 1, further comprising changing the focal depth of an imaging device from the first focal depth to the second focal depth after capturing an image at the first focal depth and before capturing an image at the second focal depth.

5. The method of claim 4, wherein changing the focal depth of the imaging device includes operating a controllably deformable mirror to change the focal depth of the imaging device from the first focal depth to the second focal depth.

6. The method of claim 4, wherein changing the focal depth of the imaging device includes controllably operating a non-adaptive optics defocus mechanism selected from a group consisting of a linearly-movable lens, , an electro-optic lens, a fluid-filled lens, and a liquid crystal device.

7. The method of claim 4, further comprising:

capturing a first plurality of images at the first focal depth;

generating a first composite image from the first plurality of images captured at the first focal depth;

capturing a second plurality of images at the second focal depth; and

generating a second composite image from the second plurality of images captured at the second focal depth,

wherein measuring the lateral difference of the position of the identified at least one individual photoreceptor includes identifying the lateral difference of the position of the identified at least one individual photoreceptor in the first composite image relative to the position of the identified at least one individual photoreceptor in the second composite image.

8. The method of claim 1, further comprising capturing an image of light reflected back from a plurality of photoreceptors at more than two focal depths.

9. The method of claim 1, further comprising:

identifying a plurality of individual photoreceptors in the image captured at the first focal depth;

identifying each photoreceptor of the plurality of photoreceptors in the image captured at the second focal depth; and

measuring a lateral difference of a position of each photoreceptor of the plurality of individual photoreceptors between the image captured at the first focal depth and the image captured at the second focal depth.

10. The method of claim 1, wherein identifying the at least one individual photoreceptor in the image captured at the first focal depth and in the image captured at the second focal depth includes performing a registration between the image captured at the first focal depth and the image captured at the second focal depth to identify the same individual photoreceptor in both the image captured at the first focal depth and the image captured at the second focal depth.

11. A system for detecting and measuring photoreceptor disarray, the system comprising:

a source positionable to project light through a pupil of an eye onto a retina of the eye;

an adjustable-focus imaging system configured to capture an image of light reflected back from a plurality of photoreceptors of the eye at a plurality of different focal depths; and

an image processing system configured to

identify an individual photoreceptor in an image captured by the adjustable-focus imaging system at a first focal depth of the plurality of focal depths,

identify the same individual photoreceptor in an image captured by the adjustable-focus imaging system at a second focal depth of the plurality of focal depths, and

measure a first lateral difference between a position of the individual photoreceptor in the image captured at the first focal depth and a position of the individual photoreceptor in the image captured at the second focal depth.

12. The system of claim 11, wherein the image processing system further configured to

identify a second individual photoreceptor in the image captured at the first focal depth,

identify the same second individual photoreceptor in the image captured at the second focal depth,

measure a second lateral difference between a position of the second individual photoreceptor in the image captured at the first focal depth and the position of the second individual photoreceptor in the image captured at the second focal depth, and

evaluating photoreceptor disarray based on a comparison of the first lateral difference and the second lateral difference.

13. The system of claim 11, wherein the adjustable-focus imaging system includes at least one imaging device selected from a group consisting of an optical-coherence tomography system, a scanning laser ophthalmoscope, and a fundus camera.

14. The system of claim 11, wherein the adjustable-focus imaging system includes an adaptive optics component selected from a group consisting of a controllably deformable mirror and a controllably deformable lens, and wherein the adjustable-focus imaging system captures images at the plurality of different focal depths by operating the adaptive optics component to change the focal depth of the imaging system from the first focal depth to the second focal depth.

15. The system of claim 11, wherein the adjustable-focus imaging system includes a lens, and wherein the adjustable-focus imaging system captures images at the plurality of different focal depths by controllably adjusting a position of the lens in a linear direction and capturing at least one image at each of a plurality of positions along the linear direction.

16. The system of claim 11, wherein the image processing system is further configured to

generate a first composite image from a first plurality of images captured by the adjustable-focus imaging system at the first focal depth, and

generate a second composite image from a second plurality of images captured by the adjustable-focus imaging system at the second focal depth,

wherein the image processing system is configured to measure the lateral difference of the position of the individual photoreceptor by identifying the lateral difference between a position of the individual photoreceptor in the first composite image and a position of the same individual photoreceptor in the second composite image.

17. The system of claim 11, wherein the image processing system is further configured to measure a plurality of lateral differences in a position of the individual photoreceptor from a

plurality of images captured by the adjustable-focus imaging system at more than two focal depths.

18. The system of claim 11, wherein the image processing system if further configured to

identify a plurality of individual photoreceptors in the image captured at the first focal depth;

identify each photoreceptor of the plurality of photoreceptors in the image captured at the second focal depth; and

measure a lateral difference of a position of each photoreceptor of the plurality of individual photoreceptors between the image captured at the first focal depth and the image captured at the second focal depth.

19. The system of claim 11, wherein the image processing system is configured to identify the individual photoreceptor in the image captured at the first focal depth and in the image captured at the second focal depth by performing a registration between the image captured at the first focal depth and the image captured at the second focal depth to identify the same individual photoreceptor in both the image captured at the first focal depth and the image captured at the second focal depth.

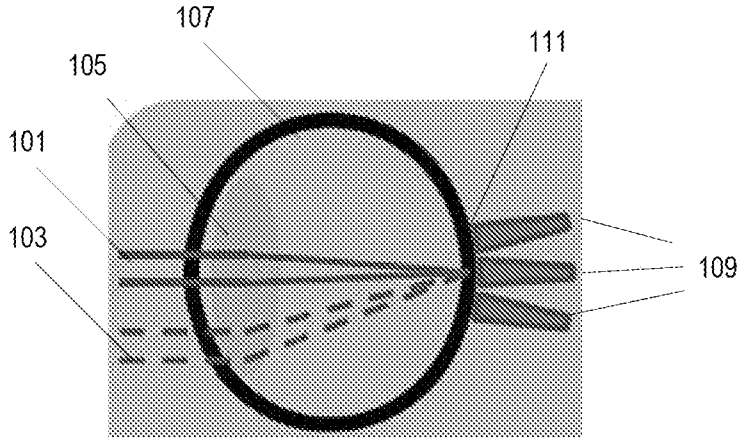
107
111
105
101
103
109

FIG. 1A

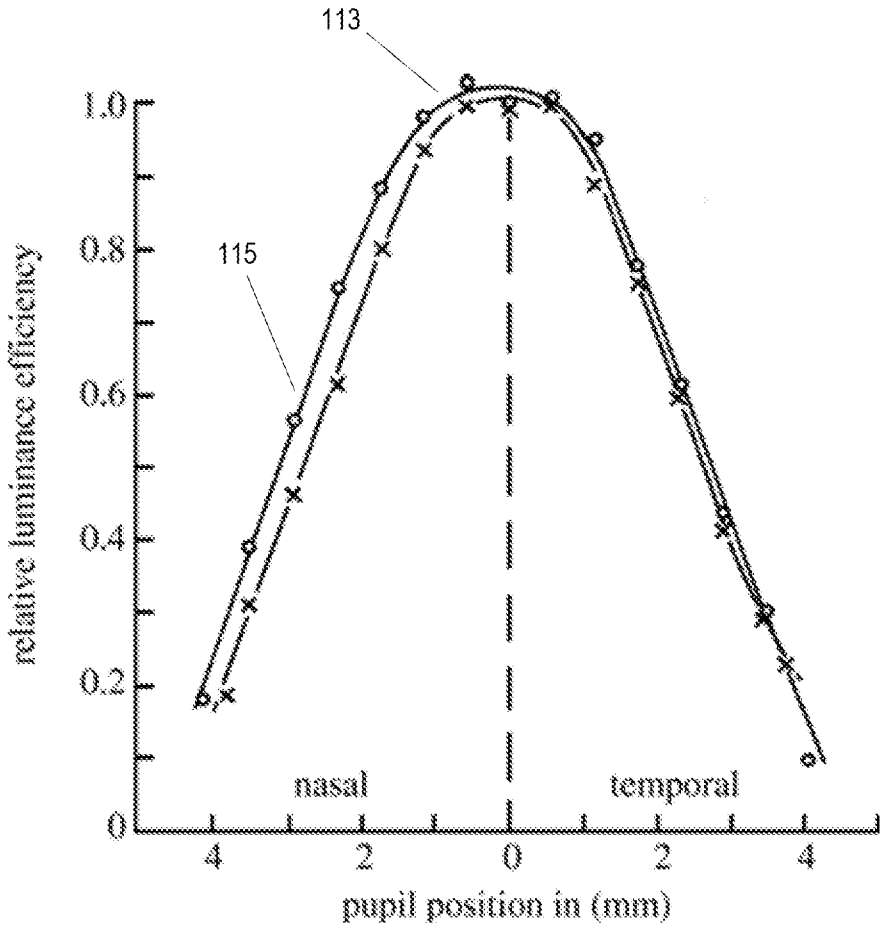
113
115
1.0
0.8
0.6
0.4
0.2
0
relative luminance efficiency
nasal
temporal
4
2
0
2
4
pupil position in (mm)

FIG. 1B

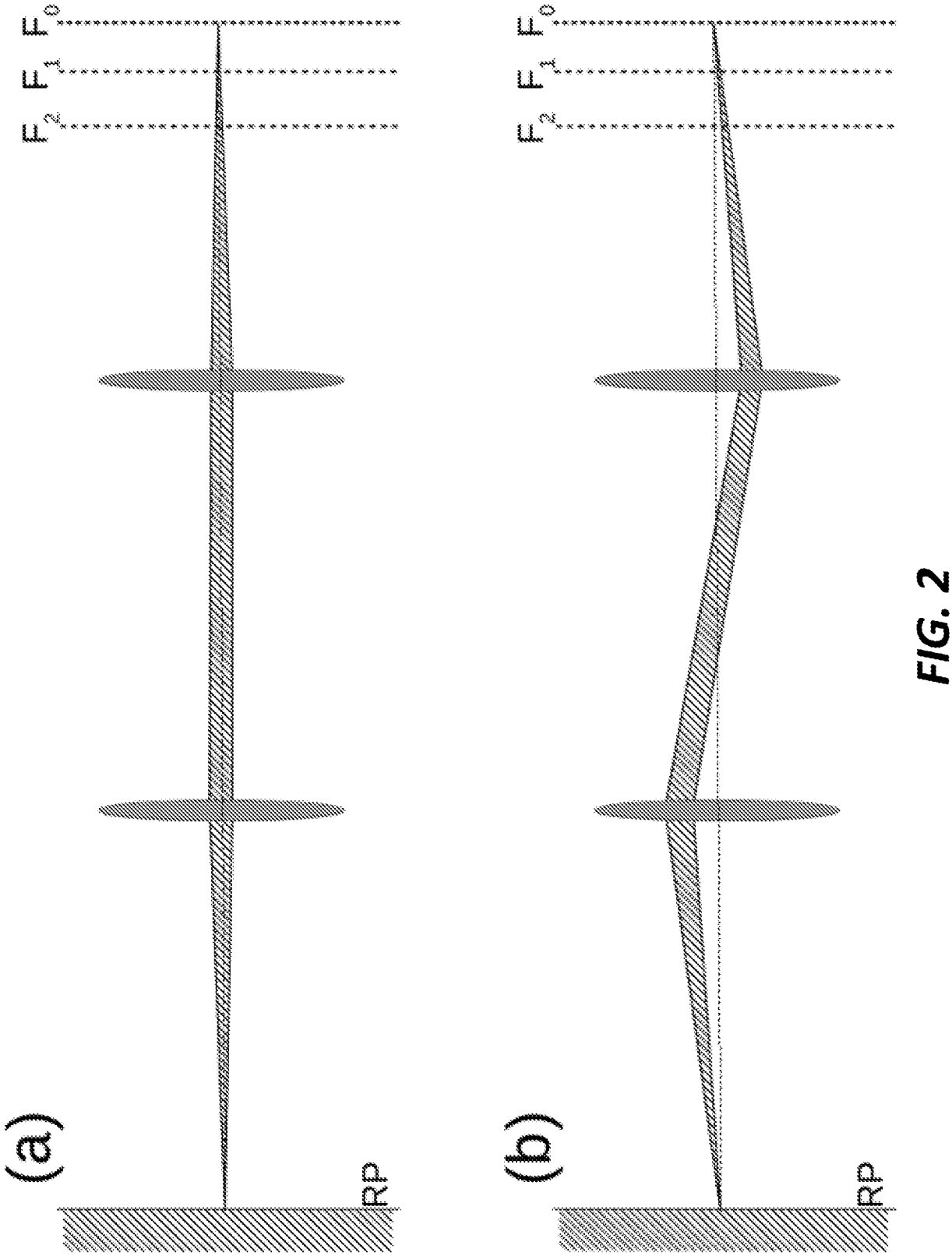

FIG. 2

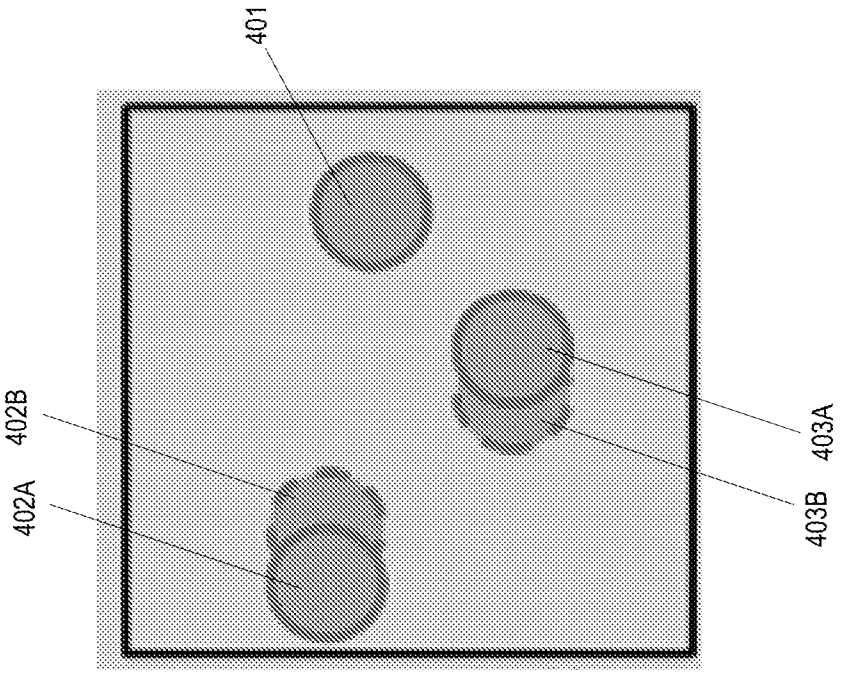

FIG. 3B

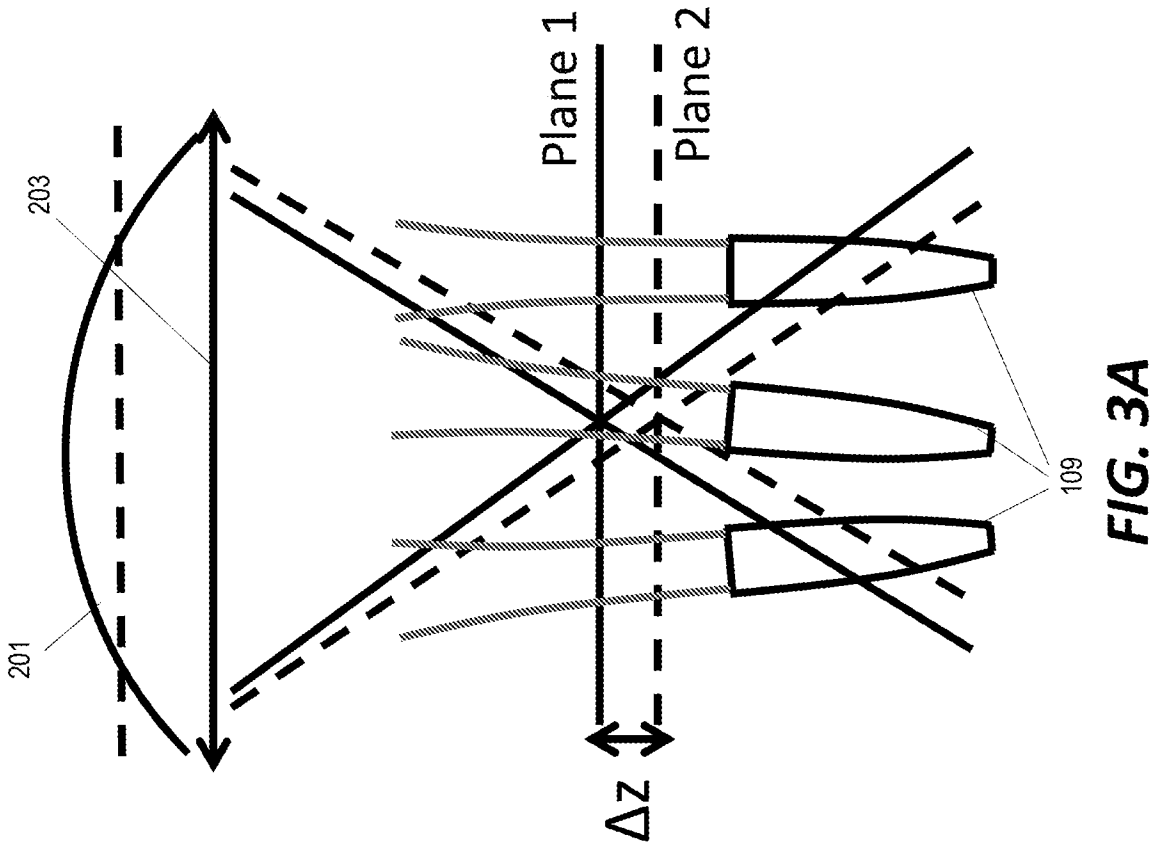

FIG. 3A

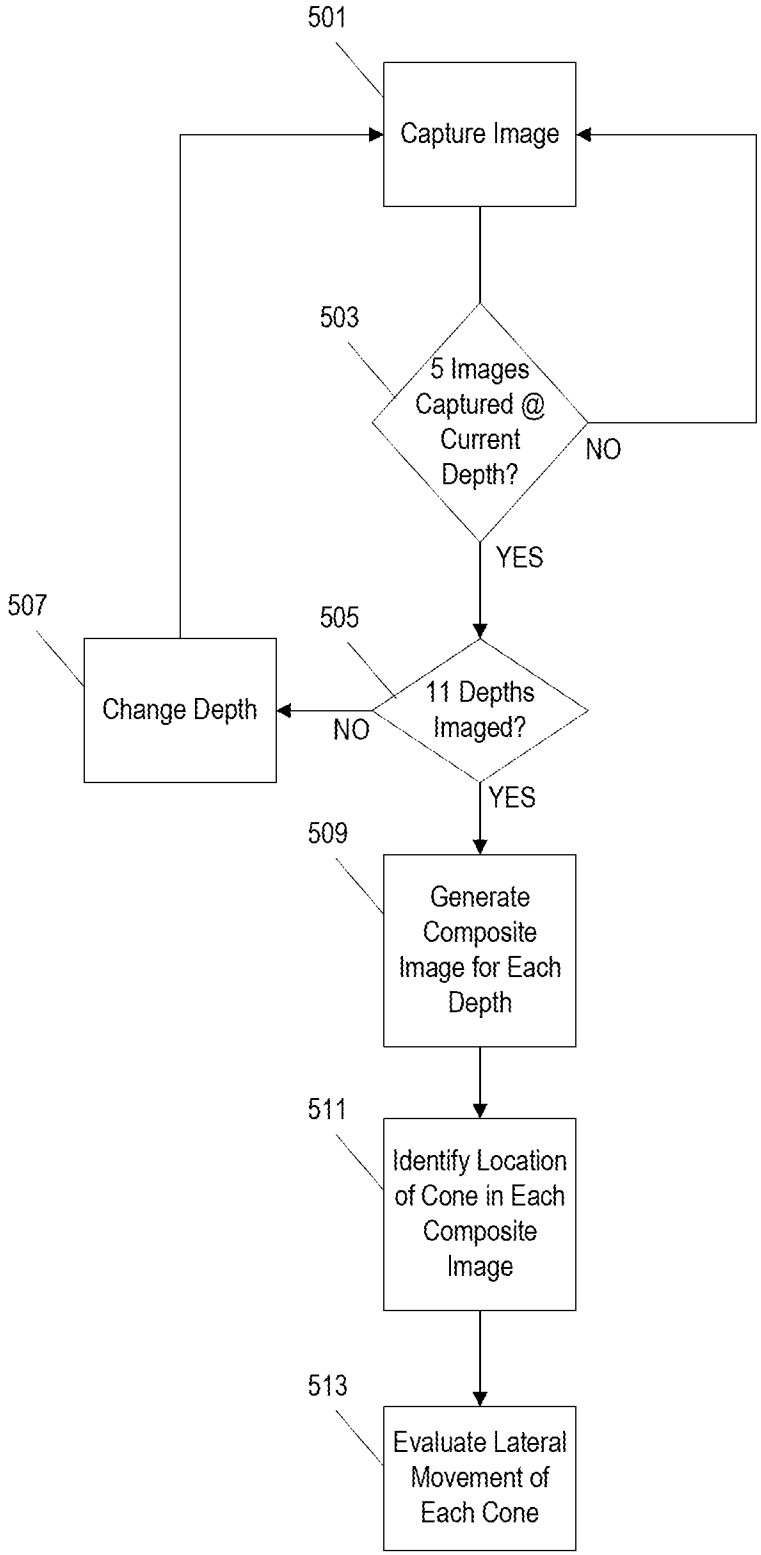
501
Capture Image
503
5 Images Captured @ Current Depth?
NO
YES
505
11 Depths Imaged?
NO
507
Change Depth
YES
509
Generate Composite Image for Each Depth
511
Identify Location of Cone in Each Composite Image
513
Evaluate Lateral Movement of Each Cone

FIG. 4

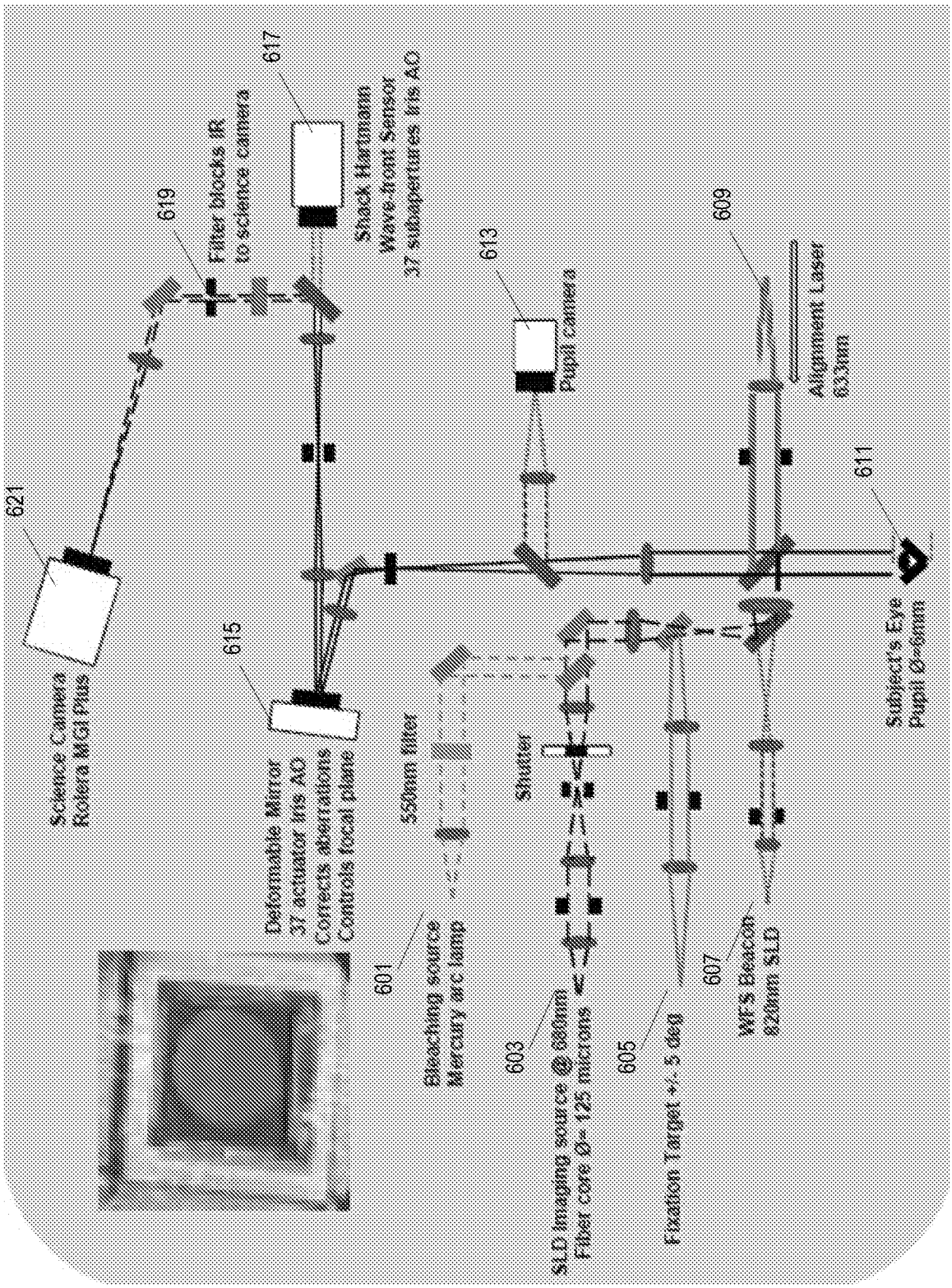
621
Science Camera
Rolera MGI Plus
619
Filter blocks IR
to science camera
617
Shack Hartmann
Wave-front Sensor
37 subapertures Iris AO
615
Deformable Mirror
37 actuator Iris AO
Corrects aberrations
Controls focal plane
613
Pupil camera
609
Alignment Laser
633nm
611
Subject's Eye
Pupil Ø~6mm
601
Bleaching source
Mercury arc lamp
550nm filter
Shutter
603
SLD imaging source @ 680nm
Fiber core Ø~ 125 microns
605
Fixation Target +/- 5 deg
607
WFS Beacon
820nm SLD

FIG. 5

INTERNATIONAL SEARCH REPORT

International application No.
PCT/US2016/029717

A. CLASSIFICATION OF SUBJECT MATTER
IPC(8) - A61B 3/02; A61B 3/00; A61B 3/02; A61B 3/12; A61B 3/14; A61B 13/00 (2016.01)
CPC - A61B 3/024; A61B 3/00; A61B 3/0008; A61B 3/0058; A61B 3/02; A61B 3/024 (2016.05)
According to International Patent Classification (IPC) or to both national classification and IPC

B. FIELDS SEARCHED

Minimum documentation searched (classification system followed by classification symbols)
IPC(8) - A61B 3/00; A61B 3/02; A61B 3/12; A61B 3/14; A61B 13/00 (2016.01)
CPC - A61B 3/00; A61B 3/0008; A61B 3/0058; A61B 3/02; A61B 3/024; A61B 3/12; A61B 3/14; A61B 13/00 (2016.05)

Documentation searched other than minimum documentation to the extent that such documents are included in the fields searched
USPC 351/209; 351/211; 351/221; 351/246; 600/558 (keyword delimited)

Electronic data base consulted during the international search (name of data base and, where practicable, search terms used)
Orbit, Google Patents, Google Scholar
Search terms used: photoreceptor, eye, optical, ocular, light, reflect, angle, depth

C. DOCUMENTS CONSIDERED TO BE RELEVANT

Category*	Citation of document, with indication, where appropriate, of the relevant passages	Relevant to claim No.
A	US 2009/0231545 A1 (PEYMAN) 17 September 2009 (17.09.2009) entire document	1-19
A	US 8,684,946 B1 (SIMS et al) 01 April 2014 (01.04.2014) entire document	1-19
A	US 2013/0128227 A1 (CALIFORNIA INSTITUTE OF TECHNOLOGY et al) 23 May 2013 (23.05.2013) entire document	1-19
A	US 6,916,096 B2 (EBERL et al) 12 July 2005 (12.07.2005) entire document	1-19
A	US 2010/0290007 A1 (VAN DE VELDE) 18 November 2010 (18.11.2010) entire document	1-19

☐ Further documents are listed in the continuation of Box C. ☐ See patent family annex.

* Special categories of cited documents:
"A" document defining the general state of the art which is not considered to be of particular relevance
"E" earlier application or patent but published on or after the international filing date
"L" document which may throw doubts on priority claim(s) or which is cited to establish the publication date of another citation or other special reason (as specified)
"O" document referring to an oral disclosure, use, exhibition or other means
"P" document published prior to the international filing date but later than the priority date claimed
"T" later document published after the international filing date or priority date and not in conflict with the application but cited to understand the principle or theory underlying the invention
"X" document of particular relevance; the claimed invention cannot be considered novel or cannot be considered to involve an inventive step when the document is taken alone
"Y" document of particular relevance; the claimed invention cannot be considered to involve an inventive step when the document is combined with one or more other such documents, such combination being obvious to a person skilled in the art
"&" document member of the same patent family

Date of the actual completion of the international search	Date of mailing of the international search report
22 June 2016	25 JUL 2016
Name and mailing address of the ISA/ Mail Stop PCT, Attn: ISA/US, Commissioner for Patents P.O. Box 1450, Alexandria, VA 22313-1450 Facsimile No. 571-273-8300	Authorized officer Blaine R. Copenheaver PCT Helpdesk: 571-272-4300 PCT OSP: 571-272-7774